Available online at https://asric.africa/engineering-sciences
ASRIC Journal of Engineering Sciences Vol.5(2)(2025) 124-145

Ensemble, Kernel-based, and Deep Learning approaches for flood susceptibility mapping: A case study at Lake-Watersheds

Sintayehu Adefires Abebe*[1], Mulu Sewinet Kerebih[1], Bewketu Assefa Mulu[1], Bekalu Weretaw Asres[1]

[1]Hydraulic and Water Resources Engineering Department, Debre Markos University, Ethiopia, sintayehu_adefires@dmu.edu.et, mulu_sewinet@dmu.edu.et, bewketu_assefa@dmu.edu.et, , bekalu_weretaw@dmu.edu.et

*Corresponding author: sintayehu_adefires@dmu.edu.et,

Received 24 April 2025; revised 16 May 2025; accepted 15 June 2025

Abstract

Lake Tana and its surrounding regions experience frequent flooding, necessitating improved susceptibility mapping to mitigate risks and enhance resilience. This study applies data-driven machine learning techniques to assess flood susceptibility utilizing data sets commonly used in large-scale river basin studies. A comprehensive flood inventory of approximately 2,080 flooded locations was compiled alongside 14 predictive variables. The predictive features include elevation, slope, distance to Lake, maximum precipitation and topographic wetness index. The models tested include Random Forest (RF), Support Vector Machine (SVM), Artificial Neural Network (ANN), and Convolutional Neural Network (CNN). Model performance was validated using the Kappa score and the area under the receiver operating characteristic curve (AUC). Results indicate that all models perform exceptionally well, with a minimum AUC of 0.87 for the testing dataset. RF consistently outperformed other models, achieving an AUC of 0.96 for the flood inventory and predictor variables. Elevation and distance to Lake Tana emerged as the most critical influencing factors. This study underscores the effectiveness of machine learning-based flood susceptibility mapping for Lake Tana and its surrounding watersheds, provided that a reliable flood inventory is available. The findings support data-driven approaches in flood risk assessment and offer valuable insights for disaster preparedness.

Keywords: Flood susceptibility; Lake Tana Basin; Machine Learning

1. Introduction

Flooding remains one of the most recurrent and devastating natural hazards affecting lives, infrastructure, and ecosystems worldwide. In Ethiopia, the socio-economic impacts of seasonal flooding have grown increasingly severe, particularly in low-lying and hydrologically sensitive basins such as Lake Tana (Alaminie *et al.*, 2023; Wubalem *et al.*, 2021). Rapid land use changes, deforestation, urban expansion, and intensifying rainfall patterns driven by climate variability have exacerbated the frequency and magnitude of flood events (Mamo *et al.*, 2019). Despite advances in regional hydrological modeling, precise flood susceptibility mapping remains a critical challenge due to data limitations, complex terrain, and nonlinear environmental drivers.

Lake Tana, Ethiopia's largest freshwater body and the source of the Blue Nile, is surrounded by a network of tributaries and floodplains that are highly vulnerable to inundation. The basin is marked by steep topographic gradients,

heterogeneous lithology, and a unimodal rainfall pattern dominated by the June–September wet season (Tesfaw *et al.*, 2024). These features drive rapid runoff generation and sediment transport, often overwhelming natural and engineered drainage systems. The frequency and spatial spread of pluvial and riverine flooding have increased in recent years due to intense rainfall, landscape alteration, and land use changes in the watersheds (Alaminie *et al.*, 2023; Weldegebriel & Amphune, 2017).

Previous studies have largely focused on deterministic or statistical modeling approaches to assess flood susceptibility in the region. For example, Wubalem *et al.* (2021) applied the analytical hierarchy process (AHP), two bivariate (information value, frequency ratio), and a multivariate (logistic regression) statistical method to model flood susceptibility in the Lake Tana subbasin. After analyzing 1,404 flood locations, they concluded that the statistical frequency method performed better than the AHP. In another study, Hiben *et al.* (2020) employed the Hydrologic Engineering Center's River Analysis System (HEC-RAS) hydraulic model and remote sensing data from the Moderate Resolution Imaging Spectroradiometer (MODIS) coupled with Geographic Information System (GIS) to map flood extent areas in the Fogera floodplain near Lake Tana. Their finding revealed that such a methodology enables a better characterization and visualization of the flood hazard. However, such deterministic or classical statistical approaches often lack spatial generalization and predictive transparency necessary for proactive flood management.

To address these limitations, the current study integrates machine learning and deep learning techniques to map flood susceptibility across the adjoining watersheds of Lake Tana using a combination of flood occurrence records and environmental conditioning factors. Random Forest (RF), Support Vector Machine (SVM), Artificial Neural Network (ANN), and Convolutional Neural Network (CNN) have emerged as powerful tools for flood susceptibility mapping due to their ability to model complex, nonlinear relationships among environmental variables (Islam & Chowdhury, 2024; M & P, 2025; Youssef *et al.*, 2022).

RF is widely praised for its robustness, interpretability, and high accuracy in handling tabular geospatial data, making it ideal for flood-prone regions with heterogeneous terrain and limited observations. RF consistently demonstrates superior performance in flood susceptibility mapping across multiple studies. Chen *et al.* (2020) found that RF outperformed other methods, achieving the highest accuracy and area under curve (AUC) values for training and validation datasets. Similarly, Habibi *et al.* (2023) reported that RF exhibited the highest performance metrics compared to Naïve Bayes. Eslaminezhad *et al.* (2022) optimized RF using binary particle swarm optimization, achieving the highest AUC among tree-based models. Ahmad *et al.* (2025) integrated hydrodynamic modeling with RF, outperforming XGBoost in prediction rate, AUC, and other evaluation metrics. These studies utilized various flood-influencing factors, including topographic, hydrological, and environmental variables. The consistent high performance of RF across diverse geographical settings highlights its robustness and effectiveness in handling complex geospatial data for flood susceptibility assessment, making it a valuable tool for flood management and prevention strategies.

Recent studies have demonstrated the effectiveness of SVM and ensemble methods for flood susceptibility mapping. Often integrated with other techniques, SVM has shown high accuracy in predicting flood-prone areas (Choubin *et al.*, 2019; Sachdeva *et al.*, 2017; Tehrany *et al.*, 2015). Ensemble approaches, combining SVM with methods like frequency ratio or particle swarm optimization, have yielded improved results compared to individual models (Sachdeva *et al.*, 2017). These studies utilize various geospatial factors, including topography, hydrology, and land use, to assess flood susceptibility. The findings highlight that key factors influencing flood prediction include distance from streams, hydrologic soil type, rainfall, elevation, and impervious surfaces (Demissie *et al.*, 2024).

In various settings, ANNs and deep learning neural networks (DLNN) have been used for flood susceptibility mapping. These approaches have shown high accuracy in handling geospatial data and predicting flood-prone areas (Ahmed *et al.*, 2022; Kalantar *et al.*, 2021; Paul, 2025; Tien Bui *et al.*, 2020). DLNN models have outperformed traditional ANNs in terms of sensitivity, specificity, and overall accuracy (Kalantar *et al.*, 2021). Integrating GIS with ANN has proven effective for flood risk analysis, achieving prediction accuracies of up to 92% (Paul, 2025; Tien Bui *et al.*, 2020). These advanced modeling techniques offer valuable flood mitigation and land-use planning tools in diverse geographical settings, including high-frequency tropical storm areas and floodplains.

Recent studies have shown the effectiveness of CNNs for flood susceptibility mapping. CNNs, particularly LeNet-5, have shown superior performance compared to traditional machine learning methods like SVM and RF (Wang *et al.*, 2020; G. Zhao *et al.*, 2020). These models handle geospatial data and can accurately identify flood-prone areas in urban catchments and regions with heterogeneous terrain (Trong *et al.*, 2023; G. Zhao *et al.*, 2020). CNN-based

approaches have achieved high accuracy scores, with AUC values ranging from 0.9 to 0.963 (Trong *et al.*, 2023; G. Zhao *et al.*, 2020). The models' robustness is evident in their ability to incorporate various flood-related factors, including precipitation, topography, and anthropogenic aspects (Youssef *et al.*, 2022; G. Zhao *et al.*, 2020). Furthermore, CNNs have improved performance in areas with limited observations and high-frequency tropical cyclones (Trong *et al.*, 2023), making them valuable tools for flood risk management and mitigation strategies.

The primary objective of this study is to evaluate and compare the performance of four machine learning and deep learning models—RF, SVM, ANN, and CNN—in predicting flood susceptibility across the adjoining watersheds of Lake Tana in Ethiopia. Using a flood inventory derived from the Global Flood Database and fourteen geospatial conditioning factors encompassing topographic, hydrologic, climatic, and proximity-based variables, the models are trained and tested to classify flood-prone and non-flood-prone zones. This research systematically assesses each algorithm's spatial precision and generalization capability by incorporating observed flood locations and detailed feature layers into model development.

To benchmark model performance, accuracy metrics including the Receiver Operating Characteristic (ROC) area under curve (AUC) and Kappa coefficient are utilized to quantify classification accuracy and agreement beyond chance. Furthermore, SHapley Additive exPlanations (SHAP) are applied to interpret feature contributions, revealing dominant flood-inducing drivers across the basin. The comparative evaluation highlights the strengths and limitations of each model, offering practical insights into their applicability for flood risk mapping in data-sparse, topographically diverse watersheds.

2. Materials and Methods

2.1. Study Area

Lake Tana, located in the northwestern highlands of Ethiopia, is the country's largest freshwater lake and the source of the Blue Nile. The Lake and its adjoining watersheds form a hydrologically dynamic region characterized by complex terrain, diverse land use, and seasonal hydrometeorological variability (Jemberie *et al.*, 2016; Teklay *et al.*, 2020). Elevations range from over 3,000 meters in the surrounding highlands to below 1,800 meters near the lake shore, creating steep gradients that influence runoff generation and flood propagation. The region's topography and expanding agricultural and urban activities intensify surface runoff and sediment transport, making it highly susceptible to flash floods and seasonal inundation.

Figure 1 shows the study area map of the Lake Tana subbasin. The main panel on the left (panel a) illustrates elevation gradients. On the right, the top inset (panel b) situates the Lake Tana region within Ethiopia and its neighboring countries. In contrast, the bottom inset (panel c) shows specific watersheds selected for flood susceptibility analysis. Black dots scattered across the study area indicate flooded locations obtained from the Global Flood Database (GFD) (Tellman *et al.*, 2021) for 2000-2018.

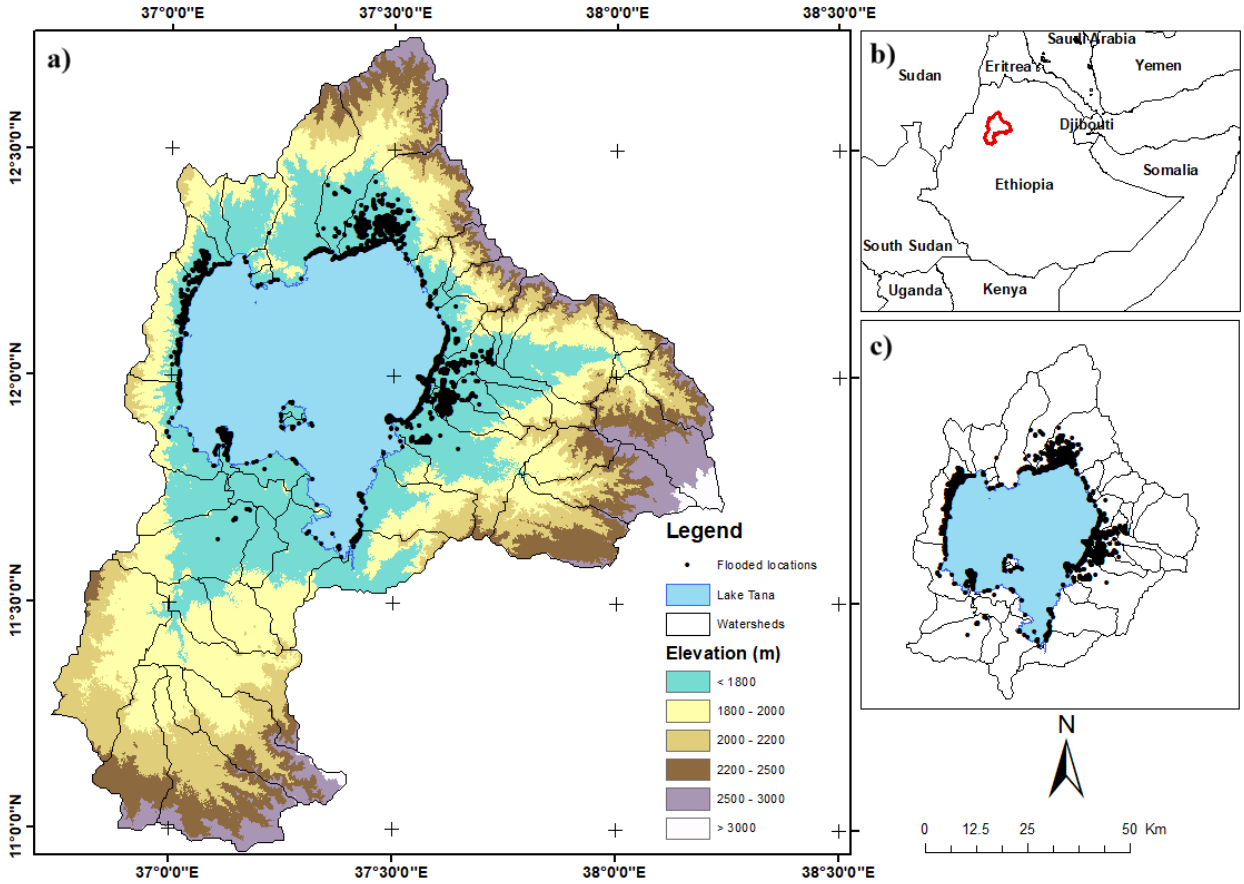

Fig. 1. (a) Location map of the study area with elevation and flood locations across the Lake Tana subbasin. (b) An inset map shows the location of the Lake Tana subbasin. (c) Map showing the selected adjoining watersheds for the study.

The Lake Tana basin experiences a unimodal rainfall regime dominated by the Inter-Tropical Convergence Zone (ITCZ), with a pronounced wet season from June to September contributing 70–90% of the annual precipitation (Abebe *et al.*, 2017). Rainfall varies spatially, with the southern catchments receiving up to 1,600 mm annually, while northern areas receive closer to 1,200 mm. This seasonal concentration of rainfall, combined with shallow lake bathymetry and limited drainage capacity, often leads to rapid water level fluctuations and localized flooding (Abebe *et al.*, 2017; Tesfaw *et al.*, 2024). Climate change projections indicate increasing precipitation and temperature trends, further exacerbating flood risks through intensified rainfall events and altered evapotranspiration dynamics (Goshu & Aynalem, 2017).

Hydrologically, the basin is fed by tributaries, with the Gilgel Abay River alone contributing approximately 60% of Lake Tana's inflow. The Lake's water balance is influenced by direct rainfall, evaporation, river inflows, and regulated outflows via the Blue Nile. Sediment deposition from upstream erosion and land degradation further complicates flood dynamics by altering channel morphology and reducing storage capacity (Alemu *et al.*, 2020; Yenehun *et al.*, 2021). These factors underscore the need for advanced geospatial and AI-driven flood susceptibility mapping to support early warning systems and sustainable watershed management.

2.2. Datasets

This study utilized two principal datasets to develop AI-driven flood susceptibility models for watersheds surrounding Lake Tana, Ethiopia. Flood inventory data and 14 flood influencing factors from various sources. Details of these datasets are given in the following sections.

2.2.1. Flood Inventory

The flood inventory was obtained from the GFD, providing spatially referenced flood occurrence across the study region. The GFD is a high-resolution (250m) archive of major flood events derived from satellite imagery, primarily utilizing NASA's MODIS data. It covers over 900 large floods worldwide from 2000 to 2018 (Tellman *et al.*, 2021). The flood events mapped in this database represent major events recorded by the Dartmouth Flood Observatory (DFO) since the beginning of the satellite records. Flood extents are mapped using a change detection algorithm applied to MODIS reflectance composites, identifying inundated areas. The dataset offers binary flood footprints ("Flooded" vs. "Not Flooded") that are temporally and spatially tagged. GFD is openly accessible through the GFD website (https://global-flood-database.cloudtostreet.info/). For this study, we compiled 2,080 flood events available for the surrounding watersheds of Lake Tana during 2000-2018 (Fig. 1(a)).

2.2.2. Flood Influencing Factors

Complementing the flood inventory, fourteen flood-influencing factors—spanning topographic, hydrologic, proximity-based, and climatic domains—were derived from diverse geospatial and remote sensing sources. These include terrain attributes such as Elevation, Slope, Aspect, and Curvature; hydrologic indicators like Curve Number (CN), Drainage Density, stream power index (SPI), topographic wetness index (TWI), and topographic roughness index (TRI); proximity metrics (distance to River/Lake); lithological classifications; and precipitation-based features (maximum precipitation and precipitation frequency). Together, these datasets enabled robust spatial learning across multiple machine learning models. Since each dataset has its own spatial resolution, we resample each to match the resolution of the flood data of the GFD (250m). The spatial maps of each factor are shown in Fig. 2.

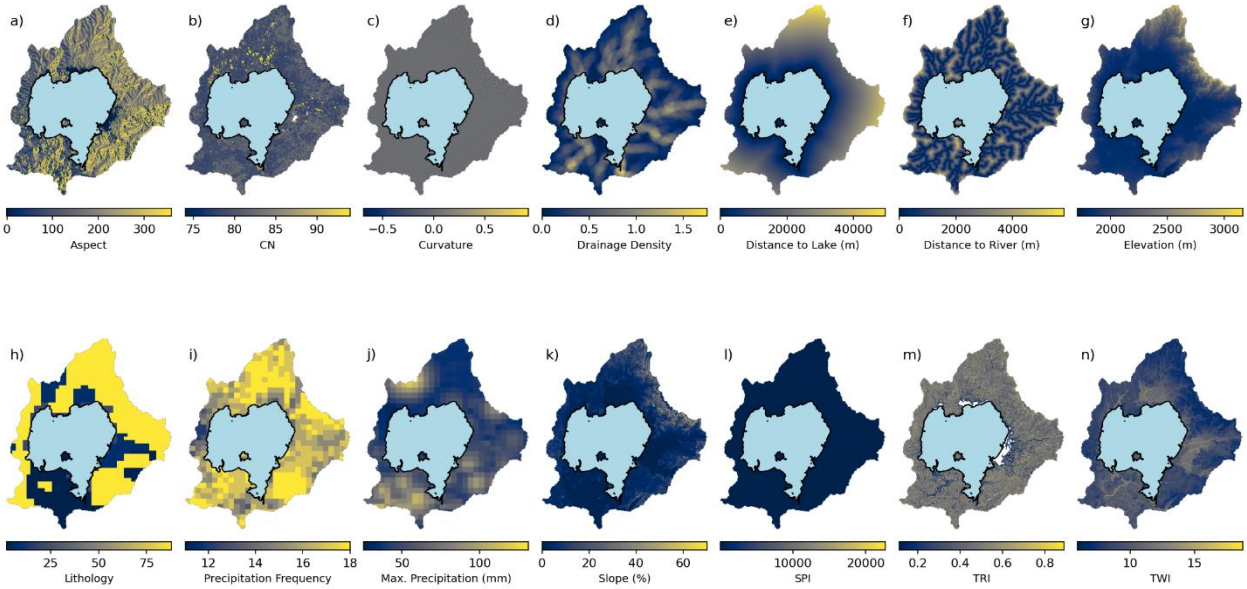

Fig. 2. Spatial distribution of flood influencing factors used to develop the models.

Elevation plays a fundamental role in flood dynamics by dictating the natural flow paths of water and the accumulation zones. Lower elevation areas are natural depressions or sinks for runoff and water pooling during high-intensity rainfall events. In contrast, higher elevations contribute less to direct inundation, although they may accelerate runoff toward flood-prone zones. In this study, we used the 90m resolution Digital Elevation Model (DEM) from the Shuttle Radar Topography Mission (SRTM) (Fig. 2(g)). The DEM is also used to derive other flood influencing factors such as aspect, slope, and curvature.

Aspect refers to the compass direction that a slope faces and influences microclimatic conditions, solar radiation exposure, and moisture retention (Geroy *et al.*, 2011). In flood modeling, aspect indirectly affects soil drying, evapotranspiration rates, and vegetation cover, all impacting infiltration and runoff generation. Slopes facing away from prevailing wind and rain directions may experience less saturation and slower runoff, while windward or shaded aspects may retain moisture and increase localized flood risk (Fan *et al.*, 2020). In this study, the aspect map was generated from the DEM using the aspect tool of Arc Map (Fig. 2(a)).

Curve number is an empirical metric that quantifies the runoff potential of an area based on land use, soil type, and hydrologic condition. High CN values (e.g., urban or compacted soils) signify reduced infiltration and elevated runoff volumes, while low values indicate better absorption and diminished flood risk. CN integrates the hydrological response to rainfall and is especially crucial in heterogeneous land-cover settings like the Lake Tana basin, where agriculture, bare soil, and urban expansion create mixed runoff behaviors. This study used the global curve number dataset called GCN250 (Jaafar *et al.*, 2019). GCN250 is derived by combining the European Space Agency global land cover dataset for 2015 (ESA CCI-LC), resampled to 250 m, and geo-registered with the hydrologic soil group global data product (HYSOGs250m). The CN map of the study area is shown in Fig. 2(b).

Curvature defines the concavity or convexity of the terrain and influences how water collects and disperses. Concave surfaces (negative curvature) tend to trap runoff, increasing flooding susceptibility, whereas convex slopes promote water dispersion and channeling. Terrain curvature provides localized clues about potential accumulation zones and complements slope and elevation data in pinpointing flood-prone depressions (Zhang *et al.*, 2023). In this study, the curvature map was generated from the DEM using the curvature tool of Arc Map (Fig. 2(c)).

Drainage density measures the total length of stream channels per unit area and reflects the efficiency of natural drainage. High drainage density suggests well-developed stream networks that rapidly convey runoff, reducing surface accumulation (Clubb *et al.*, 2016). However, if stream capacity is exceeded or blocked, these areas may become flash flood zones. Water may pond and saturate the terrain in low-density zones, leading to prolonged inundation after storms. In this study, the drainage density map was generated through the line density tool of Arc Map using the stream network of the watersheds as an input (Fig. 2(d)).

Proximity to a Lake significantly affects flood risk due to lake overflow, backwater effects, and shoreline saturation. Areas closer to the Lake are more likely to experience rising water levels during heavy rainfall and inflow events. Distance to Lake quantifies hydraulic connectivity and exposure to lacustrine flooding, especially during peak inflow seasons (Tan *et al.*, 2019). Distance to Lake Tana was calculated using the Euclidean distance tool of Arc Map (Fig. 2(e)).

Distance to the river helps assess susceptibility to fluvial flooding caused by channel overflow or poor drainage. Regions adjacent to rivers face a higher risk due to direct runoff routing and floodplain inundation. This factor also indicates how quickly runoff reaches the channel system and whether the location falls within typical backwater influence zones or overbank flood regions. Distance to river features was calculated using the Euclidean distance tool of Arc Map (Fig. 2(f)).

Lithology captures surface and subsurface materials' geological composition and structure, directly influencing infiltration, soil stability, and runoff behavior. Permeable lithologies like fractured basalts allow better drainage, reducing flood potential. In contrast, clay-rich or compacted sediments may inhibit infiltration and increase surface runoff, exacerbating flood risk in flat or concave terrains (Litwin & Harman, 2024; Lodes *et al.*, 2024). The lithological information for the study area was obtained from the Global Lithological Map (GLiM) database (Hartmann & Moosdorf, 2012). The database offers 16 major lithological classes and 12 and 14 subclasses. The lithological map of the study area is shown in Fig. 2(h).

Maximum precipitation reflects the intensity of storm events within a defined period and is a primary driver of flood initiation. Higher precipitation maxima often overwhelm drainage systems and soil storage capacities, triggering flash floods. Incorporating this variable into models ensures sensitivity to extreme rainfall events that can override terrain-based flood controls. For this study, we derived the annual maximum daily precipitation for 2000-2018 from the Enhancing National Climate Services (ENACTS) initiative data from the Ethiopian Meteorology Institute (Dinku *et al.*, 2014). The annual maximum daily precipitation map for the surrounding watersheds of Lake Tana is shown in Fig. 2(j).

Precipitation frequency indicates how often heavy rainfall events occur, contributing to cumulative saturation and antecedent wetness conditions. Frequent storms can pre-condition the soil, reduce infiltration capacity, and even cause moderate rainfall events to be flood-inducing (Cea & Fraga, 2018; Davidsen *et al.*, 2018). This variable is key in capturing seasonal flood dynamics and temporal clustering of flood events. In this study, we calculated precipitation frequency as the total number of days in a year with total precipitation exceeding the 99th percentile of the daily precipitation values during 2000-2018. The precipitation frequency map for the surrounding watersheds of Lake Tana is shown in Fig. 2(i).

Slope determines runoff velocity and the time available for water infiltration. Steeper slopes generate fast runoff and limited ponding, whereas gentle slopes allow water accumulation and increase flood risk. However, if steep slopes converge toward lowlands or poorly drained areas, they intensify flood impact by delivering runoff rapidly into vulnerable zones. In this study, the slope map was generated from the DEM using the slope tool of Arc Map (Fig. 2(k)).

SPI quantifies the erosive power of flowing water at any point in a landscape, combining local slope steepness with upstream contributing area (Micu *et al.*, 2022). High SPI values represent zones where concentrated, high-velocity runoff exerts significant mechanical force on the terrain—often leading to channel erosion, sediment mobilization, and localized flooding (Papangelakis *et al.*, 2022). In flood mapping, SPI serves as a critical geomorphic indicator of energy transfer and fluvial intensity, helping to pinpoint areas at risk of dynamic flow and overland washouts, especially in steep upland catchments feeding into Lake Tana's floodplains. The SPI map of the study area is shown in Fig. 2(l). The SPI was estimated using Equation 1.

$$SPI = A_s \tan\beta \quad (1)$$

where, SPI is stream power index, As is the basin area in $m^{2,}$ and β is the slope in radians.

TRI measures terrain irregularity and surface variability by calculating the neighboring cells' elevation variance using the DEM (Chipatiso, 2023). High TRI values indicate rugged landscapes with varied elevation changes that may channel runoff unevenly, promoting localized flooding (Trevisani *et al.*, 2023). Rough terrain can cause flow impediments and eddies, enhancing the unpredictability and spread of floodwater, especially in transition zones between uplands and flat basins. The TRI map for the Lake Tana watersheds is shown in Fig. 2(m).

TWI estimates the spatial potential for water accumulation based on the upslope contributing area and slope. High TWI values correlate with poor drainage, shallow water tables, and moisture-retentive zones—all indicative of higher flood susceptibility (Rizalihadi *et al.*, 2024). It effectively identifies catchment areas likely to experience saturation and helps delineate wetland-prone zones (Begum, 2025). The TWI map of the study area is shown in Fig. 2(n). The TWI was estimated using Equation 2.

$$TWI = \ln(A_s/\tan\beta) \quad (2)$$

where TWI is the topographic wetness index and other variables are as defined in Equation 1.

2.3. Models

In this study, we employed four diverse machine learning models—RF, SVM, ANN, and CNN—to evaluate flood susceptibility across Lake Tana's watersheds. By integrating tabular and image-based

models, the study advanced a multi-perspective, AI-driven framework for flood risk mapping. Details of the models used are given in subsequent sections. Basic components of each model are also shown in Fig. 3.

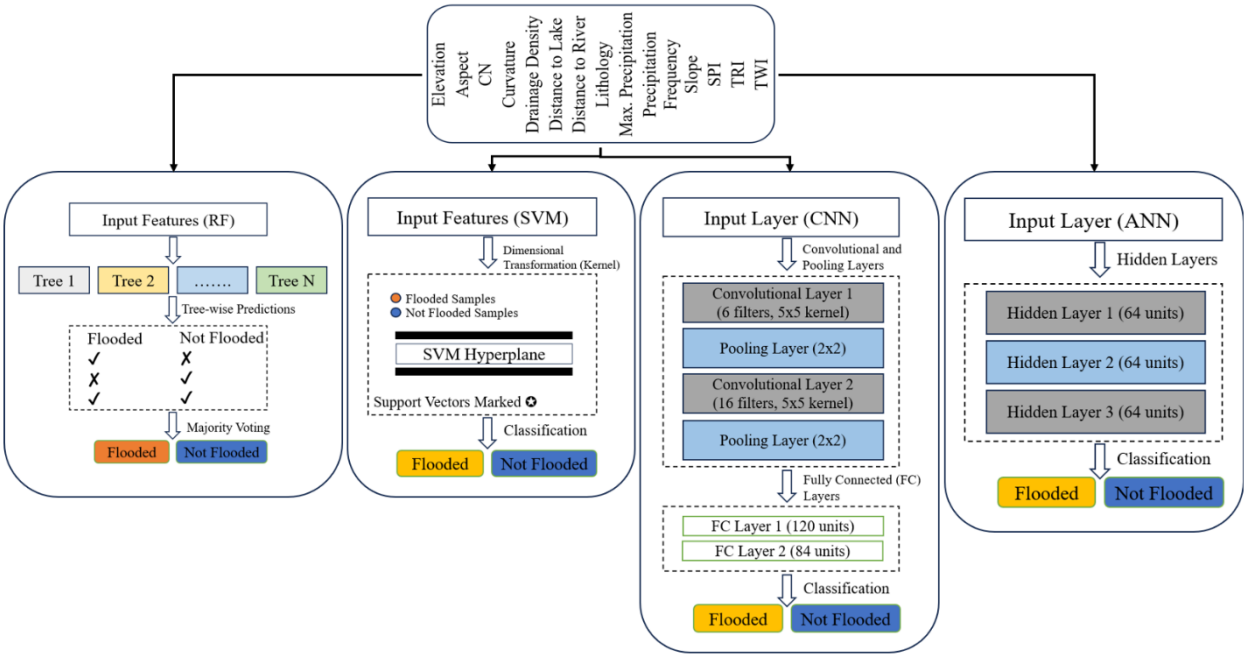

Fig. 3. An architecture schematic employed for the models used for flood classification.

2.3.1.Random Forest (RF)

RF is an ensemble learning method that combines multiple decision trees to improve prediction accuracy and reduce overfitting (Pious *et al.*, 2024). It operates by constructing trees using bootstrap samples of the training data and random feature selection at each node (Fig. 3). RF aggregates predictions through majority voting for classification or averaging for regression tasks (Svetnik *et al.*, 2003). This approach has demonstrated high accuracy across various applications, including compound classification and flood risk prediction (P. Zhao *et al.*, 2024). RF offers built-in performance assessment, feature importance measures, and the ability to handle complex, nonlinear datasets (Svetnik *et al.*, 2003; P. Zhao *et al.*, 2024). Despite challenges like high computational costs and potential biases in imbalanced datasets, RF remains a powerful and user-friendly tool in machine learning, with ongoing developments focused on improving accuracy and real-time management (Pious *et al.*, 2024).

In flood susceptibility mapping, RF handles heterogeneous tabular geospatial data such as slope, elevation, land use, and soil type. Recent studies have demonstrated the effectiveness of RF in flood susceptibility mapping (Demissie *et al.*, 2024; Habibi *et al.*, 2023). RF consistently performs well across multiple resolutions, achieving accuracies between 0.82 and 0.97 (Demissie *et al.*, 2024). Its robustness is further evidenced by high predictive power, with ROC-AUC values of 0.92 (Chakraborty *et al.*, 2024) and 0.912 (Ahmad *et al.*, 2025). In this study, RF was trained using labeled data indicating flooded and non-flooded instances, allowing the model to learn decision boundaries that correspond to terrain, climate, and hydrologic conditions.

2.3.2.Support Vector Machine (SVM)

SVM is a supervised learning model based on statistical learning theory, widely used in spatial hazard assessment (Evgeniou & Pontil, 2001). It identifies an optimal hyperplane separating flooded and non-flooded regions in a multidimensional feature space (Fig. 3). It maximizes the margin between each class's

closest points (support vectors), ensuring robust classification. For non-linearly separable data, SVM uses kernel functions to project inputs into higher dimensions where a linear separation becomes feasible.

SVM models have shown effectiveness in flood mapping and forecasting. SVM with Radial Basis Function (RBF) kernel achieved high accuracy in flood probability mapping (Baig *et al.*, 2022) and flood susceptibility prediction (Seleem *et al.*, 2022). However, some studies identified that SVM-RBF may overestimate flood extents compared to other methods like classification and regression trees (Negri *et al.*, 2025). SVM performance varies with kernel selection; linear and RBF kernels can outperform each other in different scenarios (Hong *et al.*, 2016, 2017).

2.3.3.Artificial Neural Networks (ANN)

ANN is a biologically inspired model composed of interconnected nodes (neurons) that process input features through weighted connections. In flood analysis, ANN is especially suitable for capturing nonlinear relationships and latent interactions among topographic, hydrologic, and climatic inputs (Filipova *et al.*, 2022; Paul, 2025). Studies have shown ANNs can accurately predict floods in regions with microclimatic conditions (Dhunny *et al.*, 2020) and map extreme precipitation events in semi-arid areas (Hammami & Elasmi, 2023). ANNs excel at processing continuous and categorical features, learning complex relationships between input variables and flood occurrence patterns.

For this study, we employed a DLNN proposed by (Tien Bui *et al.*, 2020). The DLNN operates through multiple hidden layers that progressively extract higher-level features from input data (Fig. 3). Each neuron receives weighted inputs, applies an activation function, and passes the result forward (Tien Bui *et al.*, 2020). During training, the network adjusts weights via backpropagation to minimize prediction error. Studies have demonstrated their effectiveness in predicting flash flood susceptibility in tropical storm areas (Tien Bui *et al.*, 2020) and flood-prone zones in floodplains (Ahmed *et al.*, 2022). DLNNs excel at modeling complex, nonlinear relationships between various factors influencing flood occurrence, including topographic, hydrologic, and climatic variables (Kalantar *et al.*, 2021). Their layered architecture enables them to capture intricate spatial interactions among these factors. Comparative analyses have shown that DLNNs achieve higher prediction accuracies than traditional methods like ANNs and SVM (Tien Bui *et al.*, 2020).

2.3.4.Convolutional Neural Networks (CNN)

CNNs are deep learning models designed to extract spatial patterns from gridded data, such as images or raster maps, with growing applications in Earth system science and ecology (Brodrick *et al.*, 2019; Nogueira *et al.*, 2015; Padarian *et al.*, 2019). They use convolutional layers to scan for local features and progressively learn complex representations through pooling and activation layers. In flood mapping, CNNs are particularly effective for detecting terrain structures and hydrological patterns that influence inundation, making them ideal for geospatial analysis with multi-band data (R.B *et al.*, 2023; Tavus *et al.*, 2022). However, application of CNNs in the context of flood susceptibility mapping is rare (G. Zhao *et al.*, 2020).

This study employed the classic CNN architecture called LeNet-5 (Lecun *et al.*, 1998). LeNet-5 is developed for handwritten digit recognition, consisting of five layers (excluding the input) that progressively extract and process spatial features (Fig. 3). It begins with an input image, which passes through a convolutional layer with six 5×5 filters, followed by an average pooling layer that downsamples the resulting feature maps. The next convolutional layer uses 16 filters with a 5x5 kernel, followed by another pooling layer. These spatial features are then flattened and passed through two fully connected layers, culminating in a sigmoid output layer that classifies the image into one of two categories (flooded vs. not flooded). This hierarchical design enables efficient feature extraction and classification, laying the groundwork for modern deep learning models (Elsaadouny *et al.*, 2020).

2.4. Performance Metrics and Feature Importance

This study evaluated model performance using the AUC and Kappa coefficient, which comprehensively assess predictive accuracy and classification reliability. AUC quantifies the ability of each model to distinguish between flooded and non-flooded zones across varying threshold settings, with higher values

indicating stronger discriminative power. The Kappa coefficient, on the other hand, accounts for the agreement between predicted and observed classifications beyond chance, offering insight into model robustness and generalization (Więckowska *et al.*, 2022). Both indices have been widely used in literature to evaluate flood susceptibility maps (Tien Bui *et al.*, 2020; G. Zhao *et al.*, 2020, 2021).

The study employed SHAP to interpret model decisions and rank predictor influence. SHAP is a game-theoretic approach that attributes the contribution of each feature to the model output. It assigns each feature a quantitative contribution to a model's prediction. It calculates the average marginal impact of a feature across all possible combinations of inputs, ensuring a fair and consistent attribution of importance. This allows for global interpretability (which features matter most) and local interpretability (why a specific prediction was made). Each SHAP value quantifies how much a specific feature pushes the prediction toward "Flooded" or "Not Flooded". SHAP has been used to explain feature importance in various flood susceptibility mapping studies(He *et al.*, 2025; Kaspi & Kuleshov, 2023; Pradhan *et al.*, 2023).

3. Results

3.1. Model Performance

This study uses ensemble, kernel-based and deep learning models to map flood-prone areas in the adjoining watersheds of Lake Tana. The methods were applied to 14 flood influencing factors to identify flooded areas. Figure 4 shows the performance of the models– evaluated using the AUC and Kappa coefficient metrics for training, validation, and test datasets.

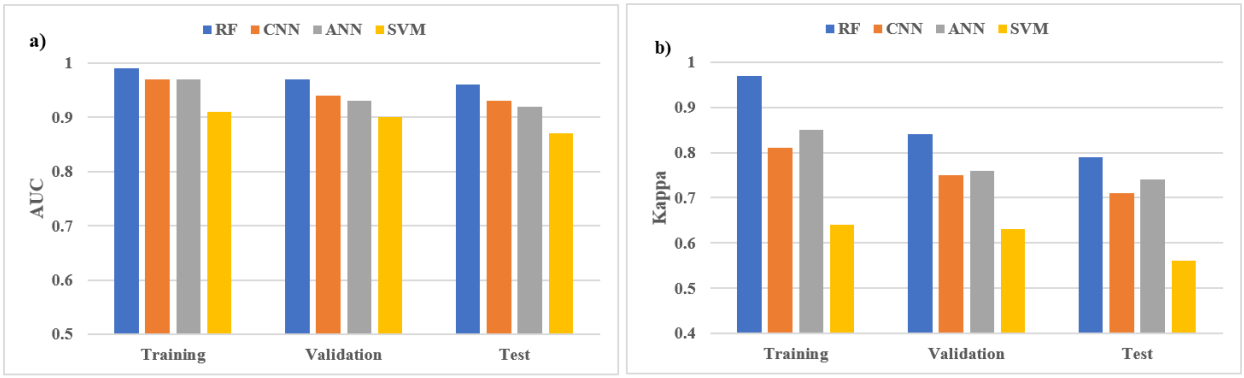

Fig. 4. Calculated performance indices for the training, validation, and test datasets using (a) AUC and (b) Kappa.

RF stands out as the most consistent and accurate model across all datasets. Its AUC scores remain high: 0.99 for training, 0.97 for validation, and 0.96 for the test sets (Fig. 4(a)). This uniformity suggests RF maintains its predictive strength while avoiding overfitting. Its Kappa scores, which measure agreement beyond chance, are also notably strong—0.97 for training, 0.84 for validation, and 0.79 for the test—reinforcing its robustness and reliability (Fig. 4(b)). CNN, ANN, and SVM all show moderate but stable AUC values around 0.90 across datasets, with CNN and ANN slightly outperforming SVM. However, despite similar AUCs, their Kappa values vary significantly. Similar studies also confirm the stronger predictive accuracy compared to CNN, ANN, and SVM (M & P, 2025; Seleem *et al.*, 2022).

Kappa coefficients reveal more about the models' classification reliability. ANN performs reasonably well, starting with a training Kappa of 0.85 and maintaining an average value of 0.75 for both validation and test sets—demonstrating balanced predictive power with minimal degradation. While matching ANN's AUC, CNN starts lower with 0.81 training Kappa and dips to 0.75 in validation and 0.71 in testing, implying mild generalization issues. By contrast, SVM shows the lowest AUC (0.87–0.91) and markedly lower Kappa values—especially for the test set (0.56)—suggesting it struggles most with correctly classifying flood-prone areas. Overall, RF combines high accuracy with interpretability and generalization, while CNN and

ANN offer promising deep learning alternatives, and SVM appears less suited to this particular flood susceptibility task.

Figure 5 shows the ROCs, which visually assess how well the models distinguish between classes for the test dataset. It plots the true positive rate (sensitivity) against the false positive rate (1-specificity). RF's curve closely approaches the plot's top-left corner, reflecting high sensitivity and low false positive rates across a threshold value of 0.5. All models except the SVM show better accuracy.

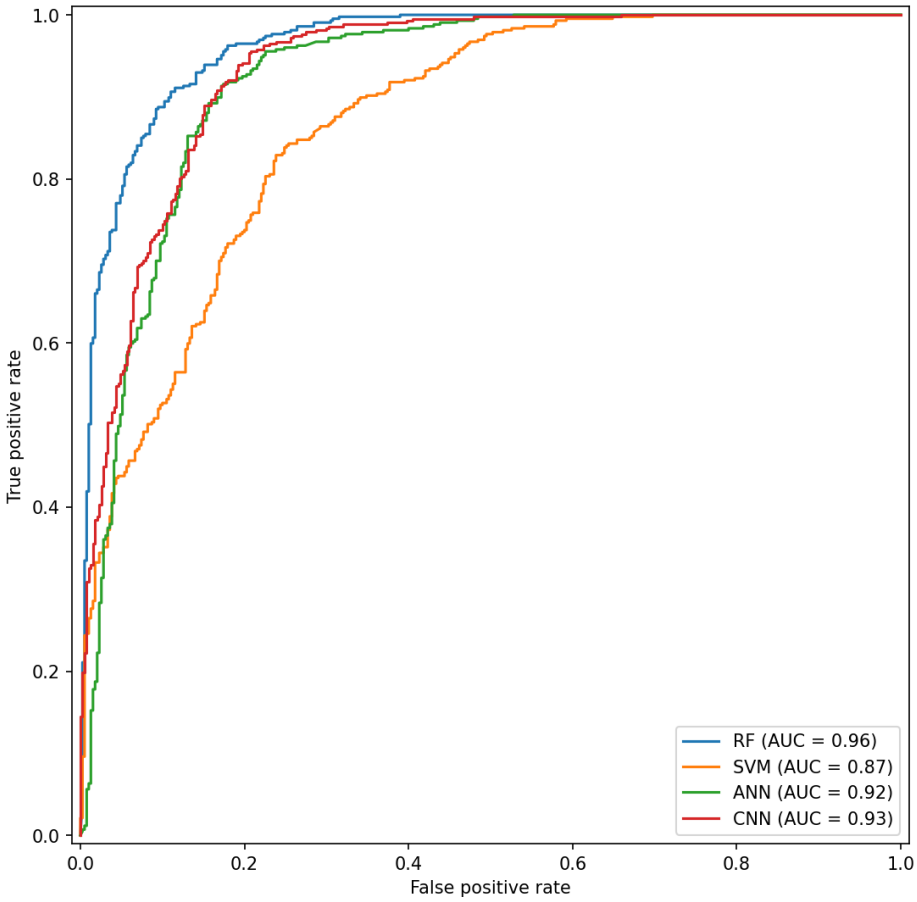

Fig. 5. ROC curve and AUC of the RF, SVM, ANN, and CNN models on the test dataset.

3.2. Flood Susceptibility Maps

The flood susceptibility maps derived from the four models are shown in Fig. 6. The maps reveal varied spatial patterns and classifications across the Lake Tana watersheds. The models' outputs were classified into five classes of flood susceptibility: very low, low, moderate, high, and very high by applying the Natural Breaks (Jenks), which is commonly employed in flood susceptibility mapping (Fang *et al.*, 2021; Khoirunisa *et al.*, 2021; Rafiei-Sardooi *et al.*, 2021; Wang *et al.*, 2020). Fig. 6 (a), representing the RF output, shows very high-risk zones concentrated near rivers and lakeshores, where most of the observed flood events are also clustered. Low-risk areas are predominantly located in elevated terrains.

The CNN-based flood susceptibility map (Fig. 6 (b)) exhibits a reasonable spatial alignment with observed flood locations. Many actual flood occurrences fall within the high and very high susceptibility zones, particularly along the lakeshore and low-elevation areas. This suggests that the LeNet-5 architecture can capture dominant geospatial patterns associated with flooding, such as terrain proximity to water bodies and drainage pathways (Pecheti *et al.*, 2025; G. Zhao *et al.*, 2020).

The ANN-based flood susceptibility map (Fig. 6 (c)) exhibits moderate agreement with observed flood points. High-risk zones—particularly those near the Lake and low-lying terrain—capture several clusters of flood occurrences, validating the ANN model's ability to extract meaningful environmental predictors. However, scattered flood points in mid- and low-risk areas indicate that the ANN may underperform in capturing certain complex terrain characteristics.

Figure 6 (d) shows the SVM-based flood susceptibility map. The result demonstrates a fair alignment with observed flood locations. Many high-risk areas identified by the model coincide with clusters of the observed flood locations, particularly around the Lake and low-lying regions. This suggests that SVM effectively captures dominant flood-prone features. However, its predictions appear slightly conservative, with several flood points scattered in moderate or low-risk zones. While sharp, the model's decision boundaries may limit its ability to generalize across complex terrain gradients (Bera *et al.*, 2022).

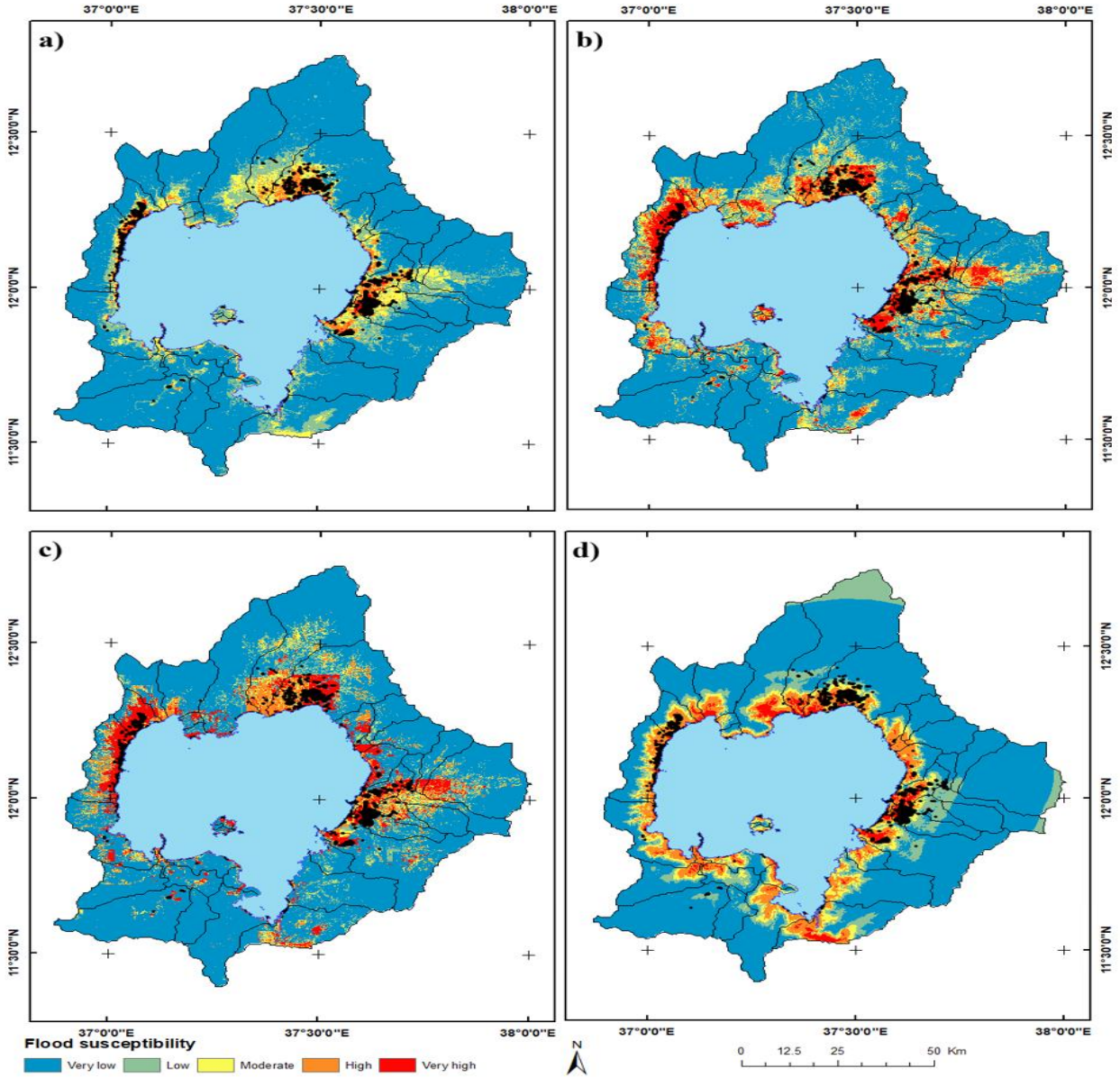

Fig. 6. Flood susceptibility map for the study area using (a) RF, (b) CNN, (c) ANN, and (d) SVM models

3.3. Feature Importance

The SHAP summary plot for the Random Forest model is shown in Fig. 7. The plot offers a granular view into the relative importance and directional impact of the 14 flood-influencing features. The results indicate that the most significant factors for the RF model are elevation, distance to Lake, TRI, slope, CN, maximum precipitation, and aspect, respectively. Elevation emerges as the most influential variable, with a wide spread of SHAP values, indicating a strong and consistent contribution to flood susceptibility prediction. Distance to Lake and TRI are closely followed, showing that proximity to Lake Tana and topographic complexity are key spatial indicators for flood susceptibility. Similarly, relatively smoother areas (lower TRI) correspond to higher predicted flood probability compared to rougher (higher TRI) areas. From a hydrologic and meteorological perspective, features like CN, maximum precipitation, and precipitation frequency show meaningful contributions, although with slightly narrower SHAP ranges for CN and precipitation frequency. Lower-ranked features such as drainage density, lithology, SPI, distance to River, and curvature exhibit relatively compressed SHAP spreads, indicating subtler but relevant contributions.

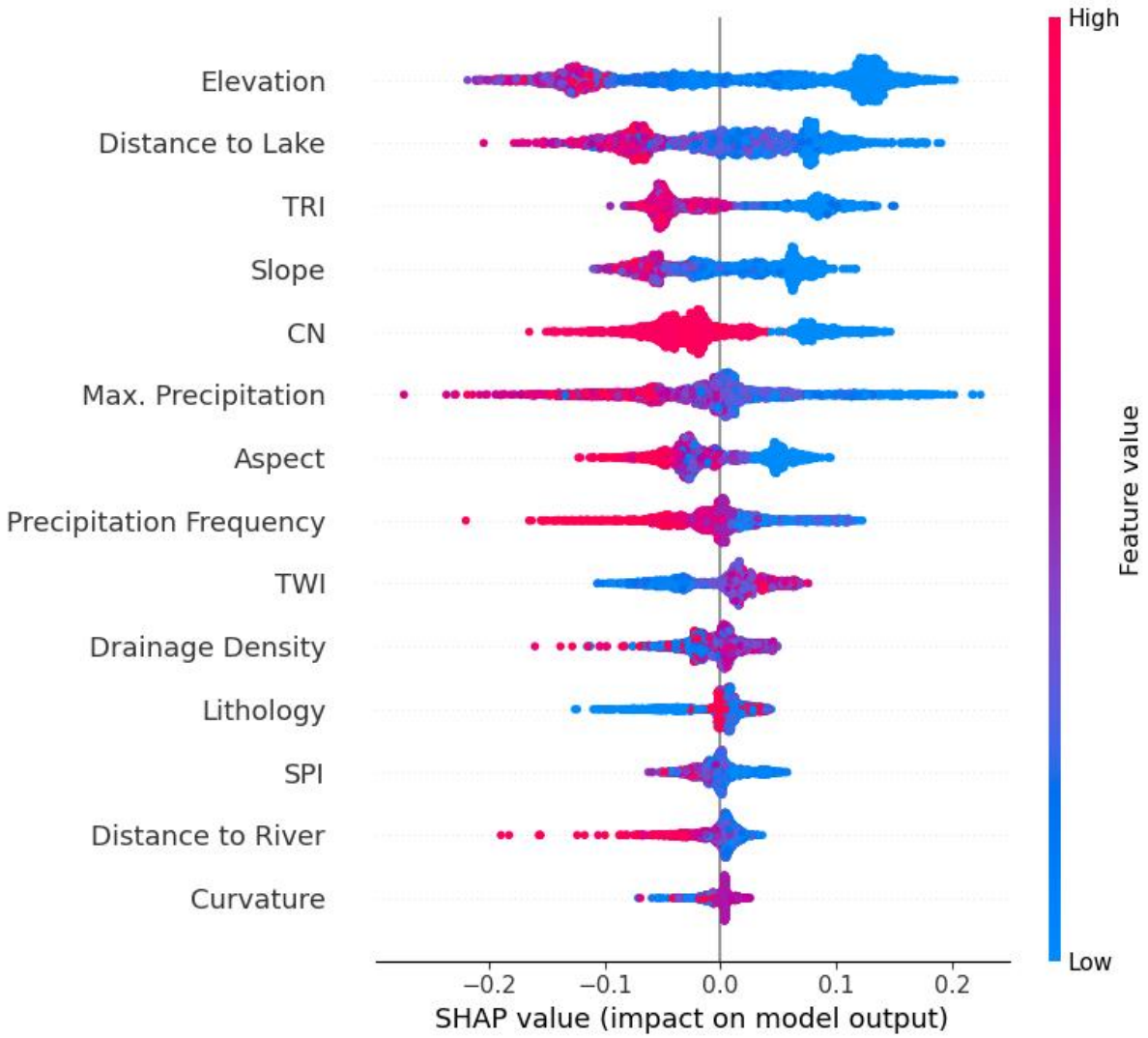

Fig. 7. SHAP values for the test dataset using the RF model.

Overall, the SHAP analysis confirms the strength of the Random Forest's interpretability, providing actionable insights into the geospatial and hydro-climatic variables most responsible for flood predictions in the Lake Tana watersheds.

4. Discussion

The performance obtained by the RF model (Fig. 5), likely stems from RF's robust handling of nonlinear relationships and its ability to leverage feature interactions and redundancies (Behr *et al.*, 2022; Ryo & Rillig, 2017). The CNN and the ANN models' ROCs suggest strong generalization capabilities, though slightly less sharp than RF. Interestingly, despite CNNs often excelling with spatial data, RF's structure and efficient learning on tabular features give it a competitive edge. The SVM, with an AUC of 0.87, trails slightly behind, possibly due to kernel limitations in capturing complex feature interactions (Roman *et al.*, 2021; Trivedi & Dey, 2013). However, its performance is still respectable, especially for data-sparse environments.

The coherence between predicted risk zones and observed flood data for the RF (Fig. 6 (a)) highlights the model's capacity to capture critical topographic, hydrologic, and proximity-based features influencing flood events. Similar studies also confirm that high-risk flood zones are predominantly clustered near rivers and low-lying areas (Adebisi Joseph Ademusire & John Adeyemi Eyinade, 2025; Zhang *et al.*, 2023). In other studies, proximity to water bodies is identified as the primary factor for flood susceptibility (Dey *et al.*, 2024; Farhadi & Najafzadeh, 2021). The CNN susceptibility map appears slightly more fragmented than the RF output, with some isolated high-risk patches and a few observed flood points falling outside the predicted high-risk areas (Fig. 6 (b)). This could be attributed to the convolutional layers focusing on localized pixel patterns rather than broader contextual relationships (Sarker *et al.*, 2019). While the model succeeds in identifying major flood-prone regions, its spatial generalization may benefit from training on more diverse terrain samples or applying post-processing smoothing. The CNN map provides a valuable, visually informative susceptibility layer that complements observation-based flood inventory data. A relatively lower accuracy is obtained for the SVM model. The Random Forest generally outperforms in spatial coherence and accuracy, encompassing most observed flood areas. Due to its pixel-sensitive architecture, CNN provides strong performance near water bodies but displays fragmentation and noise in more varied landscapes. The SVM, on the other hand, provides a less inclusive prediction. Each model brings distinct strengths, suggesting that ensemble learning or post-processing fusion could enhance overall predictive reliability.

Among the features considered, high elevations (shown in red, Fig. 7) tend to have negative SHAP values, implying lower flood risk, while lower elevations (in blue) push the model toward predicting flooding. In similar studies, elevation emerged as a critical factor in flood susceptibility prediction, with lower elevations associated with higher flood risk (He *et al.*, 2025; Kurugama *et al.*, 2023). Areas closer to the Lake are more prone to inundation, especially during peak rainfall, as they often lie within low-lying floodplains or transitional wetland zones. This spatial relationship has been consistently validated in regional flood modeling studies, where distance to water bodies emerges as a dominant predictor of flood occurrence, highlighting the Lake's influence on local drainage patterns, groundwater levels, and surface saturation. Studies of Lake Sentarum in Indonesia and Poyang Lake in China demonstrate complex inundation patterns in floodplain wetlands, with water extent and duration closely linked to rainfall patterns (Huang *et al.*, 2023; Setiawan *et al.*, 2021). At Finchaa Lake in Ethiopia, low-lying areas near the Lake were found to be at high risk of flooding, emphasizing the need for immediate mitigation measures (Nugusa Duressa & Shiferaw Regasa, 2021).

Lower CN values and less frequent precipitation events drive the model toward a flooded classification. Aspect and TWI demonstrate moderate influence, reinforcing the terrain's role in shaping water movement and accumulation. North-facing slopes (aspect values between 0 and 90 degrees) drive the model toward a flooded classification, while west-facing ones push the model toward a no-flood classification. Research

shows north-facing slopes are generally wetter and fully saturated for longer than south-facing slopes, facilitating flood accumulation (Gutiérrez-Jurado *et al.*, 2007).

Some of the lower ranked features may act as modifiers rather than primary drivers. For instance, SPI and drainage density may add refinement in differentiating moderate-risk zones, even if they are not dominant in the overall model impact. Similar results were reported by (Indra Prakash *et al.*, 2024) in a study conducted on landslide susceptibility modeling. They confirmed that factors like drainage density and SPI play a limited role in refining model predictions.

5. Conclusion

This study evaluated and compared the performance of four machine learning and deep learning models—RF, SVM, ANN, and CNN—in predicting flood susceptibility across the adjoining watersheds of Lake Tana in Ethiopia. Using a flood inventory derived from the Global Flood Database and fourteen geospatial conditioning factors encompassing topographic, hydrologic, climatic, and proximity-based variables, the models are trained and tested to classify flood-prone and non-flood-prone zones.

The results demonstrated the effectiveness of machine learning and deep learning models in mapping flood susceptibility across the Lake Tana watersheds. RF emerged as the most accurate model, achieving high AUC and Kappa scores, while CNN and ANN provided valuable spatial and nonlinear insights. SVM offered structured classification boundaries but showed limitations in capturing fragmented flood patterns. The integration of SHAP analysis further enhanced model transparency, identifying elevation and distance to Lake, TRI, slope, and CN as dominant flood drivers.

The comparative evaluation highlights the potential of AI-driven approaches to improve flood risk assessment in data-scarce and topographically complex regions. The study provides a robust framework for early warning systems, watershed planning, and climate-resilient infrastructure development by aligning model outputs with observed flood locations and interpreting feature contributions. Future work may explore ensemble modeling and temporal flood forecasting to enhance predictive reliability and operational utility.

Acknowledgments

We would like to thank the Ethiopian Meteorology Institute (EMI) for the ENACTS data used in this study.

References Cited

Abebe, W. B., G/Michael, T., Leggesse, E. S., Beyene, B. S., & Nigate, F. (2017). Climate of Lake Tana Basin. In K. Stave, G. Goshu, & S. Aynalem (Eds.), *Social and Ecological System Dynamics* (pp. 51–58). Springer International Publishing. https://doi.org/10.1007/978-3-319-45755-0_5

Adebisi Joseph Ademusire & John Adeyemi Eyinade. (2025). Geospatial machine learning for flood risk assessment in contrasting physiographic environments. *World Journal of Advanced Engineering Technology and Sciences*, *16*(1), 436–446. https://doi.org/10.30574/wjaets.2025.16.1.1232

Ahmad, I., Farooq, R., Ashraf, M., Waseem, M., & Shangguan, D. (2025). Improving flood hazard susceptibility assessment by integrating hydrodynamic modeling with remote sensing and ensemble machine learning. *Natural Hazards*, *121*(7), 7839–7868. https://doi.org/10.1007/s11069-025-07109-2

Ahmed, N., Hoque, M. A.-A., Arabameri, A., Pal, S. C., Chakrabortty, R., & Jui, J. (2022). Flood susceptibility mapping in Brahmaputra floodplain of Bangladesh using deep boost, deep learning neural network, and artificial neural network. *Geocarto International*, *37*(25), 8770–8791. https://doi.org/10.1080/10106049.2021.2005698

Alaminie, A. A., Amarnath, G., Padhee, S. K., Ghosh, S., Tilahun, S. A., Mekonnen, M. A., Assefa, G., Seid, A., Zimale, F. A., & Jury, M. R. (2023). Nested hydrological modeling for flood prediction using CMIP6 inputs around Lake Tana, Ethiopia. *Journal of Hydrology: Regional Studies*, *46*, 101343. https://doi.org/10.1016/j.ejrh.2023.101343

Alemu, M. L., Worqlul, A. W., Zimale, F. A., Tilahun, S. A., & Steenhuis, T. S. (2020). Water Balance for a Tropical Lake in the Volcanic Highlands: Lake Tana, Ethiopia. *Water*, *12*(10), 2737. https://doi.org/10.3390/w12102737

Baig, M. A., Xiong, D., Rahman, M., Islam, Md. M., Elbeltagi, A., Yigez, B., Rai, D. K., Tayab, M., & Dewan, A. (2022). How do multiple kernel functions in machine learning algorithms improve precision in flood probability mapping? *Natural Hazards*, *113*(3), 1543–1562. https://doi.org/10.1007/s11069-022-05357-0

Begum, P. N. (2025). Topographical Wetness Index of Manas River Basin, Assam, India. *Ecology, Environment and Conservation*, *31*(Suppl), S5–S13. https://doi.org/10.53550/EEC.2025.v31i02s.002

Behr, M., Wang, Y., Li, X., & Yu, B. (2022). Provable Boolean interaction recovery from tree ensemble obtained via random forests. *Proceedings of the National Academy of Sciences*, *119*(22), e2118636119. https://doi.org/10.1073/pnas.2118636119

Bera, S., Das, A., & Mazumder, T. (2022). Evaluation of machine learning, information theory and multi-criteria decision analysis methods for flood susceptibility mapping under varying spatial scale of analyses. *Remote Sensing Applications: Society and Environment*, *25*, 100686. https://doi.org/10.1016/j.rsase.2021.100686

Brodrick, P. G., Davies, A. B., & Asner, G. P. (2019). Uncovering Ecological Patterns with Convolutional Neural Networks. *Trends in Ecology & Evolution*, *34*(8), 734–745. https://doi.org/10.1016/j.tree.2019.03.006

Cea, L., & Fraga, I. (2018). Incorporating Antecedent Moisture Conditions and Intraevent Variability of Rainfall on Flood Frequency Analysis in Poorly Gauged Basins. *Water Resources Research*, *54*(11), 8774–8791. https://doi.org/10.1029/2018WR023194

Chakraborty, A., Kumar, B., & Upadhyaya, S. (2024). Predicting and Mapping Flood Susceptibility: Leveraging Explainable AI and GIS Techniques. *2024 IEEE India Geoscience and Remote Sensing Symposium (InGARSS)*, 1–4. https://doi.org/10.1109/InGARSS61818.2024.10984094

Chen, W., Li, Y., Xue, W., Shahabi, H., Li, S., Hong, H., Wang, X., Bian, H., Zhang, S., Pradhan, B., & Ahmad, B. B. (2020). Modeling flood susceptibility using data-driven approaches of naïve Bayes tree, alternating decision tree, and random forest methods. *Science of The Total Environment*, *701*, 134979. https://doi.org/10.1016/j.scitotenv.2019.134979

Chipatiso, E. (2023). Application of Geographic Information Systems in Analyzing Topographic Roughness for Nyanga District in Zimbabwe. *International Journal of Data Science and Big Data Analytics*, *3*(2), 59–65. https://doi.org/10.51483/IJDSBDA.3.2.2023.59-65

Choubin, B., Moradi, E., Golshan, M., Adamowski, J., Sajedi-Hosseini, F., & Mosavi, A. (2019). An ensemble prediction of flood susceptibility using multivariate discriminant analysis, classification and regression trees, and support vector machines. *Science of The Total Environment*, *651*, 2087–2096. https://doi.org/10.1016/j.scitotenv.2018.10.064

Clubb, F. J., Mudd, S. M., Attal, M., Milodowski, D. T., & Grieve, S. W. D. (2016). The relationship between drainage density, erosion rate, and hilltop curvature: Implications for sediment transport processes: CLUBB ET AL: DRAINAGE DENSITY. *Journal of Geophysical Research: Earth Surface*, *121*(10), 1724–1745. https://doi.org/10.1002/2015JF003747

Davidsen, S., Löwe, R., Ravn, N. H., Jensen, L. N., & Arnbjerg-Nielsen, K. (2018). Initial conditions of urban permeable surfaces in rainfall-runoff models using Horton's infiltration. *Water Science and Technology*, *77*(3), 662–669. https://doi.org/10.2166/wst.2017.580

Demissie, Z., Rimal, P., Seyoum, W. M., Dutta, A., & Rimmington, G. (2024). Flood susceptibility mapping: Integrating machine learning and GIS for enhanced risk assessment. *Applied Computing and Geosciences*, *23*, 100183. https://doi.org/10.1016/j.acags.2024.100183

Dey, H., Haque, M. M., Shao, W., VanDyke, M., & Hao, F. (2024). Simulating flood risk in Tampa Bay using a machine learning driven approach. *Npj Natural Hazards*, *1*(1), 40. https://doi.org/10.1038/s44304-024-00045-4

Dhunny, A. Z., Seebocus, R. H., Allam, Z., Chuttur, M. Y., Eltahan, M., & Mehta, H. (2020). Flood Prediction using Artificial Neural Networks: Empirical Evidence from Mauritius as a Case Study. *Knowledge Engineering and Data Science*, *3*(1), 1–10. https://doi.org/10.17977/um018v3i12020p1-10

Dinku, T., Block, P., Sharoff, J., Hailemariam, K., Osgood, D., Del Corral, J., Cousin, R., & Thomson, M. C. (2014). Bridging critical gaps in climate services and applications in africa. *Earth Perspectives*, *1*(1), 15. https://doi.org/10.1186/2194-6434-1-15

Elsaadouny, M., Barowski, J., & Rolfes, I. (2020). Extracting the Features of the Shallowly Buried Objects using LeNet Convolutional Network. *2020 14th European Conference on Antennas and Propagation (EuCAP)*, 1–4. https://doi.org/10.23919/EuCAP48036.2020.9135701

Eslaminezhad, S. A., Eftekhari, M., Azma, A., Kiyanfar, R., & Akbari, M. (2022). Assessment of flood susceptibility prediction based on optimized tree-based machine learning models. *Journal of Water and Climate Change*, *13*(6), 2353–2385. https://doi.org/10.2166/wcc.2022.435

Evgeniou, T., & Pontil, M. (2001). Support Vector Machines: Theory and Applications. In G. Paliouras, V. Karkaletsis, & C. D. Spyropoulos (Eds.), *Machine Learning and Its Applications* (Vol. 2049, pp. 249–257). Springer Berlin Heidelberg. https://doi.org/10.1007/3-540-44673-7_12

Fan, B., Tao, W., Qin, G., Hopkins, I., Zhang, Y., Wang, Q., Lin, H., & Guo, L. (2020). Soil micro-climate variation in relation to slope aspect, position, and curvature in a forested catchment. *Agricultural and Forest Meteorology*, *290*, 107999. https://doi.org/10.1016/j.agrformet.2020.107999

Fang, Z., Wang, Y., Peng, L., & Hong, H. (2021). Predicting flood susceptibility using LSTM neural networks. *Journal of Hydrology*, *594*, 125734. https://doi.org/10.1016/j.jhydrol.2020.125734

Farhadi, H., & Najafzadeh, M. (2021). Flood Risk Mapping by Remote Sensing Data and Random Forest Technique. *Water*, *13*(21), 3115. https://doi.org/10.3390/w13213115

Filipova, V., Hammond, A., Leedal, D., & Lamb, R. (2022). Prediction of flood quantiles at ungauged catchments for the contiguous USA using Artificial Neural Networks. *Hydrology Research*, *53*(1), 107–123. https://doi.org/10.2166/nh.2021.082

Geroy, I. J., Gribb, M. M., Marshall, H. P., Chandler, D. G., Benner, S. G., & McNamara, J. P. (2011). Aspect influences on soil water retention and storage. *Hydrological Processes*, *25*(25), 3836–3842. https://doi.org/10.1002/hyp.8281

Goshu, G., & Aynalem, S. (2017). Problem Overview of the Lake Tana Basin. In K. Stave, G. Goshu, & S. Aynalem (Eds.), *Social and Ecological System Dynamics* (pp. 9–23). Springer International Publishing. https://doi.org/10.1007/978-3-319-45755-0_2

Gutiérrez-Jurado, H. A., Vivoni, E. R., Istanbulluoglu, E., & Bras, R. L. (2007). Ecohydrological response to a geomorphically significant flood event in a semiarid catchment with contrasting ecosystems. *Geophysical Research Letters*, *34*(24), 2007GL030994. https://doi.org/10.1029/2007GL030994

Habibi, A., Delavar, M. R., Sadeghian, M. S., & Nazari, B. (2023). FLOOD SUSCEPTIBILITY MAPPING AND ASSESSMENT USING REGULARIZED RANDOM FOREST AND NAÏVE BAYES ALGORITHMS. *ISPRS Annals of the Photogrammetry, Remote Sensing and Spatial Information Sciences*, *X-4/W1-2022*, 241–248. https://doi.org/10.5194/isprs-annals-X-4-W1-2022-241-2023

Hammami, H., & Elasmi, S. (2023). Spatial Mapping of Extreme Precipitation Events Using Artificial Neural Networks. *2023 International Conference on Cyberworlds (CW)*, 494–495. https://doi.org/10.1109/CW58918.2023.00083

Hartmann, J., & Moosdorf, N. (2012). The new global lithological map database GLiM: A representation of rock properties at the Earth surface. *Geochemistry, Geophysics, Geosystems*, *13*(12), 2012GC004370. https://doi.org/10.1029/2012GC004370

He, F., Liu, S., Mo, X., & Wang, Z. (2025). Interpretable flash flood susceptibility mapping in Yarlung Tsangpo River Basin using H2O Auto-ML. *Scientific Reports*, *15*(1), 1702. https://doi.org/10.1038/s41598-024-84655-y

Hiben, M. G., Di Baldassarre, G., & Van Griensven, A. (2020). Can We Model Floodplain Inundation Patterns in Data-Scarce Areas? *Ethiopian Journal of Water Science and Technology*, *3*, 111–129. https://doi.org/10.59122/135811F

Hong, H., Pradhan, B., Bui, D. T., Xu, C., Youssef, A. M., & Chen, W. (2017). Comparison of four kernel functions used in support vector machines for landslide susceptibility mapping: A case study at Suichuan area (China). *Geomatics, Natural Hazards and Risk*, *8*(2), 544–569. https://doi.org/10.1080/19475705.2016.1250112

Hong, H., Pradhan, B., Jebur, M. N., Bui, D. T., Xu, C., & Akgun, A. (2016). Spatial prediction of landslide hazard at the Luxi area (China) using support vector machines. *Environmental Earth Sciences*, *75*(1), 40. https://doi.org/10.1007/s12665-015-4866-9

Huang, A., Liu, X., Peng, W., Dong, F., Han, Z., Du, F., Ma, B., & Wang, W. (2023). Spatiotemporal heterogeneity of inundation pattern of floodplain lake wetlands and impact on wetland vegetation. *Science of The Total Environment*, *905*, 167831. https://doi.org/10.1016/j.scitotenv.2023.167831

Indra Prakash, Dam Duc Nguyen, Nguyen Thanh Tuan, Tran Van Phong, & Le Van Hiep. (2024). Landslide Susceptibility Zoning: Integrating Multiple Intelligent Models with SHAP Analysis. *Journal of Science and Transport Technology*, 23–41. https://doi.org/10.58845/jstt.utt.2024.en.4.1.23-41

Islam, R., & Chowdhury, P. (2024). Local-scale flash flood susceptibility assessment in northeastern Bangladesh using machine learning algorithms. *Environmental Challenges*, *14*, 100833. https://doi.org/10.1016/j.envc.2023.100833

Jaafar, H. H., Ahmad, F. A., & El Beyrouthy, N. (2019). GCN250, new global gridded curve numbers for hydrologic modeling and design. *Scientific Data*, *6*(1), 145. https://doi.org/10.1038/s41597-019-0155-x

Jemberie, M. A., Awass, A. A., Melesse, A. M., Ayele, G. T., & Demissie, S. S. (2016). Seasonal Rainfall–Runoff Variability Analysis, Lake Tana Sub-Basin, Upper Blue Nile Basin, Ethiopia. In A. M. Melesse & W. Abtew (Eds.), *Landscape Dynamics, Soils and Hydrological Processes in Varied Climates* (pp. 341–363). Springer International Publishing. https://doi.org/10.1007/978-3-319-18787-7_17

Kalantar, B., Ueda, N., Saeidi, V., Janizadeh, S., Shabani, F., Ahmadi, K., & Shabani, F. (2021). Deep Neural Network Utilizing Remote Sensing Datasets for Flood Hazard Susceptibility Mapping in Brisbane, Australia. *Remote Sensing*, *13*(13), 2638. https://doi.org/10.3390/rs13132638

Kaspi, M., & Kuleshov, Y. (2023). Flood Hazard Assessment in Australian Tropical Cyclone-Prone Regions. *Climate*, *11*(11), 229. https://doi.org/10.3390/cli11110229

Khoirunisa, N., Ku, C.-Y., & Liu, C.-Y. (2021). A GIS-Based Artificial Neural Network Model for Flood Susceptibility Assessment. *International Journal of Environmental Research and Public Health*, *18*(3), 1072. https://doi.org/10.3390/ijerph18031072

Kurugama, K. A. K. M., Kazama, S., Chaminda, S. P., & Department of Earth Resources Engineering, University of Moratuwa, Sri Lanka. (2023). Flood susceptibility mapping using explainable machine learning models. *Proceedings of the 7th International Symposium on Earth Resources Management & Environment*, 60–67. https://doi.org/10.31705/ISERME.2023.12

Lecun, Y., Bottou, L., Bengio, Y., & Haffner, P. (1998). Gradient-based learning applied to document recognition. *Proceedings of the IEEE*, *86*(11), 2278–2324. https://doi.org/10.1109/5.726791

Litwin, D. G., & Harman, C. J. (2024). Evidence of Subsurface Control on the Coevolution of Hillslope Morphology and Runoff Generation. *Water Resources Research*, *60*(10), e2024WR037301. https://doi.org/10.1029/2024WR037301

Lodes, E., Scherler, D., Wittmann, H., Schleicher, A. M., Stammeier, J. A., Loyola Lafuente, M. A., & Grigusova, P. (2024). Influence of Lithology and Biota on Stream Erosivity and Drainage Density in a Semi-Arid Landscape, Central Chile. *Journal of Geophysical Research: Earth Surface*, *129*(11), e2024JF007684. https://doi.org/10.1029/2024JF007684

M, S., & P, S. (2025). Evaluating CNN and Random Forest Approaches for Ai-Driven Dynamic Flood Hazard Mapping. *2025 3rd International Conference on Inventive Computing and Informatics (ICICI)*, 1–5. https://doi.org/10.1109/ICICI65870.2025.11069517

Mamo, S., Berhanu, B., & Melesse, A. M. (2019). Historical flood events and hydrological extremes in Ethiopia. In *Extreme Hydrology and Climate Variability* (pp. 379–384). Elsevier. https://doi.org/10.1016/B978-0-12-815998-9.00029-4

Micu, D., Urdea, P., & Institute of Advanvces Environmental Research, West University of Timișoara, Oituz Str. 4, 300086, Timișoara, Romania. (2022). VULNERABLE AREAS, THE STREAM POWER INDEX AND THE SOIL CHARACTERISTICS ON THE SOUTHERN SLOPE OF THE LIPOVEI HILLS. *Carpathian Journal of Earth and Environmental Sciences*, *17*(2), 207–218. https://doi.org/10.26471/cjees/2022/017/215

Negri, R. G., Da Costa, F. D., Da Silva Andrade Ferreira, B., Rodrigues, M. W., Bankole, A., & Casaca, W. (2025). Assessing Machine Learning Models on Temporal and Multi-Sensor Data for Mapping Flooded Areas. *Transactions in GIS*, *29*(2), e70028. https://doi.org/10.1111/tgis.70028

Nogueira, K., Miranda, W. O., & Dos Santos, J. A. (2015). Improving Spatial Feature Representation from Aerial Scenes by Using Convolutional Networks. *2015 28th SIBGRAPI Conference on Graphics, Patterns and Images*, 289–296. https://doi.org/10.1109/SIBGRAPI.2015.39

Nugusa Duressa, J., & Shiferaw Regasa, M. (2021). Flood Inundation Mapping and Risk Analysis Case of Finchaa Lake. *American Journal of Environmental Science and Engineering*, *5*(3), 53. https://doi.org/10.11648/j.ajese.20210503.11

Padarian, J., Minasny, B., & McBratney, A. B. (2019). Using deep learning for digital soil mapping. *SOIL*, *5*(1), 79–89. https://doi.org/10.5194/soil-5-79-2019

Papangelakis, E., MacVicar, B., Ashmore, P., Gingerich, D., & Bright, C. (2022). Testing a Watershed-Scale Stream Power Index Tool for Erosion Risk Assessment in an Urban River. *Journal of Sustainable Water in the Built Environment*, *8*(3), 04022008. https://doi.org/10.1061/JSWBAY.0000989

Paul, A. (2025). Artificial neural networks for flood susceptibility analysis in Gangarampur sub-division of Dakshin Dinajpur, West Bengal, India. *Frontiers in Engineering and Built Environment*, *5*(1), 1–21. https://doi.org/10.1108/FEBE-09-2024-0061

Pecheti, S. T., U, A., K, U., & K, M. (2025). A Deep Learning Framework for Comparative Analysis in Flood Detection and Area Estimation. *2025 IEEE International Conference on Interdisciplinary Approaches in Technology and Management for Social Innovation (IATMSI)*, 1–6. https://doi.org/10.1109/IATMSI64286.2025.10984545

Pious, I. K., Rajalakshmi, A., R, P. K., C M, V., Nalini, M., & R, S. S. (2024). Enhancing Prediction Accuracy Through Random Forest in Classification and Regression. *2024 International Conference on Smart Technologies for Sustainable Development Goals (ICSTSDG)*, 1–6. https://doi.org/10.1109/ICSTSDG61998.2024.11026358

Pradhan, B., Lee, S., Dikshit, A., & Kim, H. (2023). Spatial flood susceptibility mapping using an explainable artificial intelligence (XAI) model. *Geoscience Frontiers*, *14*(6), 101625. https://doi.org/10.1016/j.gsf.2023.101625

Rafiei-Sardooi, E., Azareh, A., Choubin, B., Mosavi, A. H., & Clague, J. J. (2021). Evaluating urban flood risk using hybrid method of TOPSIS and machine learning. *International Journal of Disaster Risk Reduction*, *66*, 102614. https://doi.org/10.1016/j.ijdrr.2021.102614

R.B, Y., K.D, Y., R.S, W., & R.K, S. (2023). Automatic Flood Detection Using CNN. *International Journal of Research Publication and Reviews*, *4*(5). https://doi.org/10.55248/gengpi.4.523.44742

Rizalihadi, M., Meilianda, E., Yulianur, A., & Away, Y. (2024). Identification of spatial potential flood-prone area using topographic wetness index under the digital elevation model of Kr. Keureuto watershed, North Aceh. *Journal of Physics: Conference Series*, *2916*(1), 012009. https://doi.org/10.1088/1742-6596/2916/1/012009

Roman, I., Santana, R., Mendiburu, A., & Lozano, J. A. (2021). In-depth analysis of SVM kernel learning and its components. *Neural Computing and Applications*, *33*(12), 6575–6594. https://doi.org/10.1007/s00521-020-05419-z

Ryo, M., & Rillig, M. C. (2017). Statistically reinforced machine learning for nonlinear patterns and variable interactions. *Ecosphere*, *8*(11), e01976. https://doi.org/10.1002/ecs2.1976

Sachdeva, S., Bhatia, T., & Verma, A. K. (2017). Flood susceptibility mapping using GIS-based support vector machine and particle swarm optimization: A case study in Uttarakhand (India). *2017 8th International Conference on Computing, Communication and Networking Technologies (ICCCNT)*, 1–7. https://doi.org/10.1109/ICCCNT.2017.8204182

Sarker, C., Mejias, L., Maire, F., & Woodley, A. (2019). Flood Mapping with Convolutional Neural Networks Using Spatio-Contextual Pixel Information. *Remote Sensing*, *11*(19), 2331. https://doi.org/10.3390/rs11192331

Seleem, O., Ayzel, G., De Souza, A. C. T., Bronstert, A., & Heistermann, M. (2022). Towards urban flood susceptibility mapping using data-driven models in Berlin, Germany. *Geomatics, Natural Hazards and Risk*, *13*(1), 1640–1662. https://doi.org/10.1080/19475705.2022.2097131

Setiawan, F., Ridwansyah, I., & Subehi, L. (2021). Identification of Rainfall and Inundation pattern using remotely sensed data in Lake Sentarum Floodplain Area. *Indonesian Journal of Limnology*, *2*(2), 9–20. https://doi.org/10.51264/inajl.v2i2.16

Svetnik, V., Liaw, A., Tong, C., Culberson, J. C., Sheridan, R. P., & Feuston, B. P. (2003). Random Forest: A Classification and Regression Tool for Compound Classification and QSAR Modeling. *Journal of Chemical Information and Computer Sciences*, *43*(6), 1947–1958. https://doi.org/10.1021/ci034160g

Tan, Z., Wang, X., Chen, B., Liu, X., & Zhang, Q. (2019). Surface water connectivity of seasonal isolated lakes in a dynamic lake-floodplain system. *Journal of Hydrology*, *579*, 124154. https://doi.org/10.1016/j.jhydrol.2019.124154

Tavus, B., Can, R., & Kocaman, S. (2022). A CNN-BASED FLOOD MAPPING APPROACH USING SENTINEL-1 DATA. *ISPRS Annals of the Photogrammetry, Remote Sensing and Spatial Information Sciences*, *V-3–2022*, 549–556. https://doi.org/10.5194/isprs-annals-V-3-2022-549-2022

Tehrany, M. S., Pradhan, B., & Jebur, M. N. (2015). Flood susceptibility analysis and its verification using a novel ensemble support vector machine and frequency ratio method. *Stochastic Environmental Research and Risk Assessment*, *29*(4), 1149–1165. https://doi.org/10.1007/s00477-015-1021-9

Teklay, A., Dile, Y. T., Asfaw, D. H., Bayabil, H. K., & Sisay, K. (2020). *Modeling the Impact of Climate Change on Hydrological Responses in the Lake Tana Basin, Ethiopia*. https://doi.org/10.21203/rs.2.19829/v1

Tellman, B., Sullivan, J. A., Kuhn, C., Kettner, A. J., Doyle, C. S., Brakenridge, G. R., Erickson, T. A., & Slayback, D. A. (2021). Satellite imaging reveals increased proportion of population exposed to floods. *Nature*, *596*(7870), 80–86. https://doi.org/10.1038/s41586-021-03695-w

Tesfaw, B. A., Dzwairo, B., & Sahlu, D. (2024). Climate variability, trend, and associated risks: Tana sub-basin, Ethiopia. *Journal of Water and Climate Change*, *15*(3), 1282–1299. https://doi.org/10.2166/wcc.2024.577

Tien Bui, D., Hoang, N.-D., Martínez-Álvarez, F., Ngo, P.-T. T., Hoa, P. V., Pham, T. D., Samui, P., & Costache, R. (2020). A novel deep learning neural network approach for predicting flash flood susceptibility: A case study at a high frequency tropical storm area. *Science of The Total Environment*, *701*, 134413. https://doi.org/10.1016/j.scitotenv.2019.134413

Trevisani, S., Teza, G., & Guth, P. L. (2023). Hacking the topographic ruggedness index. *Geomorphology*, *439*, 108838. https://doi.org/10.1016/j.geomorph.2023.108838

Trivedi, S. K., & Dey, S. (2013). Effect of feature selection methods on machine learning classifiers for detecting email spams. *Proceedings of the 2013 Research in Adaptive and Convergent Systems*, 35–40. https://doi.org/10.1145/2513228.2513313

Trong, N. G., Quang, P. N., Cuong, N. V., Le, H. A., Nguyen, H. L., & Tien Bui, D. (2023). Spatial Prediction of Fluvial Flood in High-Frequency Tropical Cyclone Area Using TensorFlow 1D-Convolution Neural Networks and Geospatial Data. *Remote Sensing*, *15*(22), 5429. https://doi.org/10.3390/rs15225429

Wang, Y., Fang, Z., Hong, H., & Peng, L. (2020). Flood susceptibility mapping using convolutional neural network frameworks. *Journal of Hydrology*, *582*, 124482. https://doi.org/10.1016/j.jhydrol.2019.124482

Weldegebriel, Z. B., & Amphune, B. E. (2017). Livelihood resilience in the face of recurring floods: An empirical evidence from Northwest Ethiopia. *Geoenvironmental Disasters*, *4*(1), 10. https://doi.org/10.1186/s40677-017-0074-0

Więckowska, B., Kubiak, K. B., Jóźwiak, P., Moryson, W., & Stawińska-Witoszyńska, B. (2022). Cohen's Kappa Coefficient as a Measure to Assess Classification Improvement following the Addition of a New Marker to a Regression Model. *International Journal of Environmental Research and Public Health*, *19*(16), 10213. https://doi.org/10.3390/ijerph191610213

Wubalem, A., Tesfaw, G., Dawit, Z., Getahun, B., Mekuria, T., & Jothimani, M. (2021). Comparison of statistical and analytical hierarchy process methods on flood susceptibility mapping: In a case study of the Lake Tana sub-basin in northwestern Ethiopia. *Open Geosciences*, *13*(1), 1668–1688. https://doi.org/10.1515/geo-2020-0329

Yenehun, A., Dessie, M., Azeze, M., Nigate, F., Belay, A. S., Nyssen, J., Adgo, E., Van Griensven, A., Van Camp, M., & Walraevens, K. (2021). Water Resources Studies in Headwaters of the Blue Nile Basin: A Review with Emphasis on Lake Water Balance and Hydrogeological Characterization. *Water*, *13*(11), 1469. https://doi.org/10.3390/w13111469

Youssef, A. M., Pradhan, B., Dikshit, A., & Mahdi, A. M. (2022). Comparative study of convolutional neural network (CNN) and support vector machine (SVM) for flood susceptibility mapping: A case study at Ras Gharib, Red Sea, Egypt. *Geocarto International*, *37*(26), 11088–11115. https://doi.org/10.1080/10106049.2022.2046866

Zhang, X., Kang, A., Ye, M., Song, Q., Lei, X., & Wang, H. (2023). Influence of Terrain Factors on Urban Pluvial Flooding Characteristics: A Case Study of a Small Watershed in Guangzhou, China. *Water*, *15*(12), 2261. https://doi.org/10.3390/w15122261

Zhao, G., Pang, B., Xu, Z., Cui, L., Wang, J., Zuo, D., & Peng, D. (2021). Improving urban flood susceptibility mapping using transfer learning. *Journal of Hydrology*, *602*, 126777. https://doi.org/10.1016/j.jhydrol.2021.126777

Zhao, G., Pang, B., Xu, Z., Peng, D., & Zuo, D. (2020). Urban flood susceptibility assessment based on convolutional neural networks. *Journal of Hydrology*, *590*, 125235. https://doi.org/10.1016/j.jhydrol.2020.125235

Zhao, P., Zhai, M., & Qi, H. (2024). Machine Learning-Based Flood Risk Prediction: An Analysis of the Effectiveness of Random Forest Models. *2024 3rd International Conference on Smart City Challenges & Outcomes for Urban Transformation (SCOUT)*, 47–51. https://doi.org/10.1109/SCOUT64349.2024.00020

Figures

List of Abbreviations

AHP	Analytical Hierarchy Process
AI	Artificial Intelligence
ANN	Artificial Neural Network
AUC	Area Under Curve
CN	Curve Number
CNN	Convolutional Neural Network
DEM	Digital Elevation Model
DFO	Dartmouth Flood Observatory

DLNN	Deep Learning Neural Networks
ENACTS	Enhancing National Climate Services
GCN250	Global Curve Number of 250m resolution
GFD	Global Flood Database
GIS	Geographic Information System
GLiM	Global Lithological Map
HEC-RAS	Hydrologic Engineering Center's River Analysis System
ITCZ	Inter-Tropical Convergence Zone
MODIS	Moderate Resolution Imaging Spectroradiometer
RBF	Radial Basis Function
RF	Random Forest
ROC	Receiver Operating Characteristic
SHAP	SHapley Additive exPlanations
SPI	Stream Power Index
SRTM	Shuttle Radar Topography Mission
SVM	Support Vector Machine
TRI	Topographic Roughness Index
TWI	Topographic Wetness Index